J. Agr. Sci. Tech. (2017) Vol. 19: 97-111

Encapsulation of Iranian Garlic Oil with *β*-cyclodextrin: Optimization and its Characterization

Kh. Khoshtinat[1], M. Barzegar[1], M. A. Sahari[1], and Z. Hamidi[1]

ABSTRACT

The aim of this study was to optimize the encapsulation conditions of Garlic Oil (GO) with *β*-cyclodextrin (GO/β-CD) inclusion complex by the co-precipitation method. Response surface optimization of encapsulation of GO with *β*–CD was performed with a three-variable, three-level and the optimum conditions were as follows: temperature: 35°C, Core/Wall: 8/100, and Wall/Solvent: 5.5/100. The complex was characterized by different techniques including UV–visible spectroscopy, Fourier transform infrared spectroscopy, X-ray diffractometry, and differential scanning calorimetry. Spectroscopic techniques and morphological analysis by Scanning Electron Microscope (SEM) confirmed formation of GO/*β*-CD. The *in vitro* release profile of GO from the GO/*β*-CD complex at different pH values (1.5, 4, 5.5, and 6.5) at 37°C showed that the maximum and minimum release of GO after two days were 36.59% at pH 6.5, and 1.12% at pH 4, respectively. In simulation of gastrointestinal tract, the maximum and minimum release of GO were in colon (10.29%), and stomach (0.60%), respectively. Therefore, GO/*β*-CD complex could be suggested in formulation of food systems such as salad dressing and sausage.

Keywords: *Allium sativum* L., Garlic oil, *In-vivo* release, Response surface method, SEM.

INTRODUCTION

Garlic (*Allium sativum* L. Family Liliaceae) is a widely distributed plant and cultivated (1,437,690 hectare) all over the world (Petrovska and Cekovska, 2010). Iran is the 16th in the world ranking of garlic production, with about 50% raising production in 2013 (Anonymous a, 2013).

There are no significant pharmacological activities of garlic at normal human consumption (2-5 g d^{-1}). Also, the essential Oil of Garlic (GO) is specific, which is produced from thiosulfates during the steam treatment, but does not exist in the whole plant (Rainy *et al.*, 2014).

GO contains organosulfur compounds such as DiAllyl Sulfide (DAS), DiAllyl DiSulfide (DADS), DiAllyl TrisSulfide (DATS), DiAllyl TetraSulfide (DATTS), and ajoene, decomposition products of allicin, which contribute to its antimicrobial, antioxidant, anticarcinogenic properties (Siow and Ong, 2013). GO is Generally Recognized As Safe (GRAS) natural products by FDA, but because of being volatile, water insoluble, having low physicochemical stability, very pungent flavor, and strong odor (900 times more than fresh garlic), its application in food industry is limited (Anonymous b, 2016; Wang *et al.*, 2011). It should be diluted in vegetable oil or used in encapsulated form (Santhosha *et al.*, 2013).

Inclusion complex can increase the solubility limit of the undesired odors, and protects it against light-induced reactions, oxidation, sublimation, volatilization and heat-promoted decomposition (Zhang *et al.*, 2015; Marques, 2010). Among three major types of CDs, *β*-CD is the most widely used, because of its relatively suitable cavity volume and reasonable price, and it has been on the GRAS list since 1998 (Zhang *et al.*, 2015; Anonymous b, 2016). Many varieties of

[1]Department of Food Science and Technology, Faculty of Agriculture, Tarbiat Modares University, P. O. Box: 14155-336, Tehran, Islamic Republic of Iran.
*Corresponding author; e-mail: mbb@modares.ac.ir

[DOR: 20.1001.1.16807073.2017.19.1.10.5]

organic compounds, which enter entirely or partly into the relatively hydrophobic cavity of CD, could form inclusion complex with it. Various essential oils, flavors, and some other compounds have been reported to form inclusion complex with *β*-CD such as cinnamon thyme (Peggy *et al.*, 2010), eugenol (Seo *et al.*, 2010), cholesterol (Fauziah *et al.*, 2013), *trans*-cinnamaldehyde, eugenol, cinnamon bark, and clove bud extracts (Hill *et al.*, 2013), naringenin (Yang *et al.*, 2013), rutin (Nguyen *et al.*, 2013), sweet orange flavor (Zhu *et al.*, 2014), and *trans*-anethole (Zhang *et al.*, 2015). The inclusion complex of *β*-CDs heightened the possibility of increasing the solubility and stability of garlic oil and controlling its release rate. There is no evidence to show the effect of encapsulation variables such as temperature and core to wall ratio on inclusion complex yield, or loading.

The objective of this study was the encapsulation of Iranian garlic oil using the co-precipitation method and its optimization by RSM method. We also aimed to analyze the inclusion complex of GO with *β*-CD by different analytical techniques including UV–visible spectroscopy, Differential Scanning Calorimetry (DSC), Fourier Transform-Infrared Spectroscopy (FT-IR), and XRD. Another objective was to carry out *in vitro* studies to determine release characterization GO/*β*-CD complex in different pH buffer system, and also in different simulated human gastrointestinal tract (gastric, mixture of gastric and intestinal, intestinal, and colonic fluids).

MATERIALS AND METHODS

Materials

Garlic Oil (GO) was kindly supplied by Magnolia Flavor & Fragrance Company (Kaveh industrial city, Iran), and was stored at 4^{o}C. Beta-CycloDextrin (β-CD, Cat No. C4767 minimum 98%) and enzymes including pepsin and pancreatin (containing lactose (as extender), trypsin, amylase, lipase, ribonuclease, and protease) were purchased from *Sigma*-Aldrich Co. (USA). All other chemicals and solvents were analytical grade and used without purification.

Chemical Composition of Garlic Essential Oils

GO was subjected to gas chromatography-mass spectrometry (GC/MS) analysis on an Agilent 6890 GC-5973 MS system (Agilent, DE, USA). Analysis was carried out at 70 eV and 20^{o}C. The capillary column was BPX5 with a 30 m length, an interior diameter of 0.25 mm, and a film thickness of 0.25 μm. The carrier gas was helium at flow rate of 0.5 mL min^{-1}. The oven temperature was programmed from 50 to 300^{o}C. An initial temperature was 50^{o}C, held for 5 minutes, increasing at 3 ^{o}C min^{-1}, until reaching 300^{o}C, then, held for 3 minutes. Injection temperature was 290^{o}C (by split 1 to 25), source temperature of ionization 220^{o}C (Electron ionization method), scan span 40 to 500, and Chemstation software. Quantitative data were obtained by the electronic integration of the FID peak areas. The components of the GO were identified by comparison of their mass spectra and indices, using those published in the literature (Adams, 2001; McLafferty and Stauffer, 1989), and all samples were run in duplicate.

Preparation of GO and *β*-CD Complex

The inclusion complex of *β*-CD and GO was prepared by using a co-precipitation method described by Wang *et al.* (2011) with minor modification. In a double-wall glass container, connected with a circulating bath, a defined weight (±0.001 g) of *β*-CD was dissolved in 20 mL ethanol/distilled water (1/2, v/v) mixture and maintained at 60^{o}C on a magnetic hot stirrer. After cooling the *β*-CD solution to definite temperature, a portion of GO dissolved in ethanol (1:2, v/v), was added slowly with continuous agitation. The resultant mixture was put in an ultrasonic bath (TECNO-GAZ, SPA, Italy) at 80W for 4 hours, then, stored overnight at cooling temperature (4°C). GO/*β*-CD complex was obtained by using vacuum-filtration and membrane filter (Millipore 0.45 μm HATF

[DOR: 20.1001.1.16807073.2017.19.1.10.5]

filter, mixed cellulose acetate). To clear excessive GO on the surface of *β*-CD, the precipitate was washed twice with ethanol, dried in a vacuum oven (Memmert, Germany) at 40°C until a constant weight was reached. The final powders were packaged in amber glass bottles, and stored in an airtight glass desiccator at room temperature. The inclusion ratio of GO and total recovery was calculated as follows:

Inclusion ratio (%)= [GO content of inclusion complex (mg)/Initial GO (mg)]×100 (1)

Total recovery (%) = Recovered powder/Initial (β –CD+GO)×100 (2)

Optimization of GO/*β*-CD Complex Preparation

Response Surface Methodology (RSM) was employed for investigating the effect of three factors including encapsulation temperature (F1), GO: *β*-CD ratio or core/wall (F2), and *β*-CD: Solvent ratio or wall/solvent (F3) on the encapsulation of GO with *β*-CD. A three-level-three-factor, Central Composite Face centered (CCF) was employed in this optimization study (Table 1). Total Recovery (TR, R1), Inclusion ratio (IR, R2), and GO loading (GOL, R3) were taken as the responses. All the experiments were randomly carried out in order to minimize the effect of unexplained variability in the observed responses due to systematic errors. To optimize the three individual factors in the design, 34 runs were carried out and the data were analyzed by using the Design-Expert 7.0.0. ANOVA was used to analyze the model for significance and suitability, after that, three additional confirmation experiments were conducted to verify the validity of the statistical experimental strategies.

Quantification of GO in the Inclusion Complex

GO (5.0 mg) was dissolved into absolute ethanol (50 mL). Then, serial dilutions were prepared by making up 1.0, 2.0, 4.0, 6.0, 8.0, 10.0 and 12.0 mL solution to 25 mL with absolute ethanol, and their absorbance were monitored by a UV-Vis Spectrophotometer (Agilent Cary 60, CA. USA), using cell with 1 cm path length, at 210 nm, which was found by scanning from 200 to 800 nm. The concentration (X) and the absorbance (Y) of GO had a good relationship as a straight line, when the concentration of GO was < 30 μg mL^{-1}. The regression equation was as follows:

$Y= 0.062X+0.0235$, $R^2= 0.9993$

The content of GO in the inclusion complex was determined using the method described by Wang *et al.* (2011) and Zhang *et al.* (2015). A 20-30 mg of GO/*β*-CD complex and 30 mL of absolute ethanol were added to a 50 mL stoppered conical flask, placed in an ultrasonic cleaner (SONO, SW12H Switzerland) at 1,000W for 10 minutes. After centrifuging at 2,500 rpm for 10 minutes (Sigma 3K30 Centrifuge, UK), the supernatant containing GO was analyzed using ultraviolet spectrophotometer at 210 nm by the calibration curve of GO.

Physicochemical Characterization

UV–Visible Spectroscopy

GO, *β*-CD, and their inclusion complex (GO/β-CD) were analyzed by UV–visible spectrophotometer, recording UV–visible absorption spectrum. Cyclohexane and water

Table 1. Coded levels for factors used in experimental design for encapsulation of GO with B-CD.

Factors	Coded X_1	Coded level		
		-1	0	1
Temperature (°C)	F1	30	40	50
GO: B-CD (core/wall) ratio	F2	8	10	12
B-CD: Solvent (wall/solvent) ratio	F3	3	5	7

[DOR: 20.1001.1.16807073.2017.19.1.10.5]

were used to dissolve GO and *β*-CD, respectively. GO/*β*-CD was added to cyclohexane (1: 10 w/v) and the mixture was gently shaken for 20 minutes. Subsequently, all solvent phases were separated by centrifugation (4,500 rpm, 20 minutes, at room temperature), and scanned in the range of 200 to 400 nm (Wang *et al.*, 2011).

Fourier Transform-Infrared Spectroscopy (FT-IR)

The FT-IR spectra of GO, *β*-CD, and GO/*β*-CD were collected in the frequency range between 4,000 and 500 cm^{-1} on Nicolet IR 100 FT-IR thermo-scientific spectrophotometer (Nicolet, USA) with 256 scans at a resolution of 4 cm^{-1}. As samples should be moisture free, GO was mixed with a little portion of sodium sulfate and centrifuged (9,000 rpm, 10 minutes, at 16^{o}C). GO/*β*-CD and *β*-CD were dried in a vacuum oven at 40^{o}C until the weight was constant. The samples were mixed in potassium bromide (KBr) powder and pellets were made to perform the measurements. GO was fixed on KBr plates. GO/*β*-CD and *β*-CD were ground with spectroscopic grade KBr powder and then pressed (10000 psi pressure) into1 mm pellets (2 mg of sample per 200 mg dry KBr). A blank KBr disc was used as background. By using the software of the spectrophotometer, baseline was automatically corrected and FT-IR spectra were smoothed.

Differential Scanning Calorimetry (DSC)

DSC analysis for GO, *β*-CD, and GO/*β*-CD was carried out with a Shimadzu DSC-60 differential calorimeter calibrated with indium (Shimadzu, Japan). Each sample (4–7 mg) was heated in a crimped aluminum pan at a scanning rate of 5 ^{o}C min^{-1} between 10 and 300^{o}C under a nitrogen flow of 40 mL min^{-1} for *β*-CD, and GO/*β*-CD, and 30 mL min^{-1} for GO. The reference was an empty pan sealed in the same way. Reproducibility was tested by analyzing the samples in triplicate.

X-Ray Diffractometry (XRD)

The X-ray powder diffraction patterns were obtained using X-Ray diffractometer (XRD, X'Pert MPD, Philips, Netherlands) equipped with Ni filtered CuKα radiation (λ= 1.54056Å) source operated at a voltage of 40 kV and a 30 mA current. GO, *β*-CD, and GO/*β*-CD were previously dried at 110^{o}C for 24 hours. Samples were placed on a zero-background silicon holder (PhilipsPW1812) to avoid any disturbing and also the background signal. Surface was covered by an adhesive (zinc powder) and scanned in the *2θ* angle range between 10 and 80^{o} with a scan rate of 8° min^{-1}, and a step size of 0.02^{o}. All samples were analyzed in triplicate.

Morphological Analysis

The morphological characteristics of *β*-CD, and GO/*β*-CD were observed by scanning electron microscope (SEM, Model KYKY EM 3200, Beijing, China) at 500, 2,500 and 5,000, and also 40,000 times magnification for the former and latter cases, respectively. Samples were attached to SEM aluminum stubs via a 2-sided adhesive tape. As the samples had no electrical conductivity, they were coated with a thin layer of gold by using Sputter-coater (Model SBC 12). Afterwards, it was examined using SEM set at 26 kV. The SEM photographs Images with magnifications of 500, 2,500, and 5,000 for *β*-CD and 40,000 for GO/*β*-CD were prepared.

Release of GO from the Produced Inclusion Complex

pH Buffer System

GO/*β*-CD is very stable at room temperature. By increasing temperature, an obvious increase in release rate was observed (Wang *et al.*, 2011). Therefore, the release of GO from inclusion complex at 37^{o}C (body temperature) was investigated at four pH, including 1.5 (0.05M sodium chloride solution), 4 (acetate buffer), 5.5, and 6.5 (phosphate buffers), according to the method described by Haroun and El-Halawany (2010). Speed and time of centrifugation, volume

[DOR: 20.1001.1.16807073.2017.19.1.10.5]

of buffer, buffer to test tube volume ratio, test tube shaking speed, content of inclusion complex to buffer volume ratio were studied based on one factor at a time. The released GO was increased by rising of the centrifuge speed and time, and decrease in inclusion complex to buffer volume ratio. Test tube shaking speed and buffer to test tube volume ratio were optimized at 200 rpm and 2:3, respectively.

Briefly, 40 mg GO/*β*-CD was mixed with 20 mL of each buffer and placed in a shaking incubator. Samples of the release medium were taken out, at intervals, and the amount of GO released was determined at 210 nm. After each estimation, the volume was replaced with the fresh buffer. These studies were carried out in triplicate.

Simulated Human Gastrointestinal Tract

Release of GO from GO/*β*-CD in simulated human gastrointestinal tract (four dissolution media) was studied by using USP dissolution test apparatus with paddle stirring (ERWEKA GmbH, Heusenstamm, Germany). This was performed by stirring 500 mL of each medium at 100 rpm, and 37 ± 0.1^{o}C including Simulated Gastric Fluid (SGF) at pH 1.2 [containing HCl (37%), 4 mL; NaCl, 0.11 g; and pepsin, 1.78 g] for 1 hour; Simulated Intestinal Fluid (SIF) at pH 7.4 (containing 0.2N NaOH, 105 mL; KH_2PO_4, 3.78 g; and pancreatin, 5.55 g) for 2 hours hours; mixture of simulated gastric and intestinal fluid at pH 4.5 (mixing SGF pH 1.2 and SIF pH 7.4 in a ratio of 36:64) for 2 hours; Simulated Colonic Fluid (SCF) at pH 7.0 (containing 0.1M Phosphate-Buffered Saline, or PBS) for 3 hours. Samples were withdrawn every 15 minutes for SGF, 30 minutes for SIF and mixture of SGF and SIF, and 45 minutes for SCF in equal content and replaced with fresh dissolution media (Pu *et al.*, 2011*)*. The samples were filtered through syringe filter (Millex LG 0.22 µm), and GO content was determined spectrophotometrically at 210 nm (the wavelength which was found by scanning of SGF, SIF, mixture of SGF and SIF, and SCF from 200 to 800 nm).

RESULTS AND DISCUSSION

Chemical Composition of GO

Two major Iranian GO constituents were diallyldisulphide (41.33%) and diallyltrisulfide (28.82%). Methyl allyl sulfide and allyl sulfide were next in rank with 7.83 and 6.65%, respectively (Table 2). Evidences demonstrate that GO volatiles content vary according to different factors including agronomic and genetic factors of the plant source. For instance, diallyldisulphide content differs in

Table 2. Iranian garlic oil composition determined by GC.

Components	RT	KI	%
1,2-Dithiolane	7.97	851	0.25
Allyl sulfide	8.40	861	6.65
Disulfide,methyl 2-propenyl	11.19	924	0.07
Methyl allyl sulfide	13.52	969	7.83
Diallyldisulphide	19.72	1089	41.33
3-Vinyl-1,2-dithiocyclohex-4-ene	25.44	1204	1.66
3-Vinyl-1,2-dithiocyclohex-5-ene	26.77	1232	3.74
Diallyltrisulfide	30.65	1316	28.82
Terisulfide,di-2-propenyl	30.83	1320	0.33
7-chloro-s-triazola(1,5-c)pyrimidin-5(1h)one	34.24	1397	2.18
2-(2-Thia-4-pentenyl)-1-thia-cyclohex-5-ene	39.99	1536	0.12
Diallyltetrasulphide	40.99	1561	3.93
4,5-Dimethyl-thiazole	49.15	1780	0.61
1,3-Butadiene,3-methyl-1,1-bis(methylthio)	50.08	1807	0.30
Total		98.17	

[DOR: 20.1001.1.16807073.2017.19.1.10.5]

Cameroonian garlic (37.3%), Chinese garlic (35%), Moroccan garlic (23.2%), French garlic (21.8%), and Mexican garlic (17.2%). The contents of diallyltrisulfide were 49.6, 42.0, 57.4, 24.2, and 26.4%, respectively (Anonymous c, 2016; Anonymous d, 2013; Douiri *et al.*, 2013).

Optimization of GO/*β*-CD Complex Preparation

Response Surface Methodology (RSM) is one of the multivariate techniques which can deal with experimental design and statistical modeling. Thirty four runs were conducted for optimizing the three individual factors including temperature (A), core/wall (B), and wall/solvent (C) on the encapsulation of GO with *β*-CD. The optimal conditions for the encapsulation of garlic oil as core material with *β*-CD as wall material was temperature 35°C, core/wall as 8/100, and wall/solvent as 5.5/100.

Validation of Optimized Conditions

Three additional experiments were carried out at these optimal conditions in order to compare the predicted results with experimental results. The experimental total recovery (82.1±0.28%), inclusion ratio (90.71±0.46%), and GO loading (11.88±0.27%) were close to the predicted values (80.10, 89.35, and 11.55%, respectively). Thus, for predicting the maximum total recovery Central Composite Face centered (CCF) was considered as an accurate tool.

Total Recovery

ANOVA showed that responses of total recovery (A) ranged from 61.86 to 83.83 %, and ratio of max to min was 1.35516. The model *F*-value of 12.08 signified the model was significant. Final equation for total recovery was found as follows:

Total recovery= [(+95.93253–0.32160)×(Temperature–1.64075)×(Core/Wall+1.58050)×Wall]/Solvent

Total recovery decreased when temperature and core/wall increased, although the effect of temperature was less than the other. By increasing the wall/solvent, total recovery increased.

Inclusion Ratio

The results of ANOVA for the inclusion ratio (B) indicated that response ranged from 39.49 to 97.34% and ratio of max to min was 2.46493. The model *F*-value of 4.43 showed the model was significant.

Final equation for inclusion ratio was found as follows (non-significant numbers were omitted):

Inclusion ratio= [(-71.60940+8.71307)×(Temperature+1.66506)×(Core/Wall+0.59783)×Wall]/ Solvent

By increasing the temperature, inclusion ratio increased up to about 40°C, after which increase in temperature decreased the inclusion complex formation. When core to wall ratio increased, inclusion ratio decreased. By increasing the wall to solvent ratio, inclusion ratio increased up to about 5:100, then increasing of core to wall ratio decreased the formation of inclusion complex. The effect of increasing of core to wall ratio on decreasing of inclusion ratio was more than increasing wall to solvent ratio on decreasing the formation of inclusion complex.

Garlic Oil Loading

Based on the results of ANOVA for the garlic oil loading (C), response ranged from 4.9 to 14.0%, and ratio of max to min was 2.86531. The model *F*-value of 5.50 showed the model was significant. Final equation for garlic oil loading was found as follows:

Garlic oil loading= [(+8.89-1.24)×(Temperature-1.33)×(Core/Wall+0.67)×Wall]/Solvent

By increasing the temperature, garlic oil loading decreased. Also, increase in core to wall ratio caused decrease in garlic oil loading. When wall to solvent ratio increased, garlic oil loading increased too.

[DOR: 20.1001.1.16807073.2017.19.1.10.5]

Physicochemical Characterization of Produced Complex

UV–Visible Spectroscopy

GO, *β*-CD, and GO/*β*-CD (containing the same content of GO) were scanned in the range of 200 to 400 nm. There was no UV absorption for *β*-CD in water. In the spectrum of GO in cyclohexane solution, the λ max value was found at 225 nm, which may be imputed to the linear diallyl group in GO (Figure 1). The cyclohexane extract of GO/*β*-CD had negligible GO concentration comparing with GO in cyclohexane solution. These results indicated that GO could form an inclusion complex with *β*-CD**.** Wang *et al.* (2011) showed that the UV absorption peak was not observed in the spectrum of the cyclohexane extract of GO/*β*-CD complex at 210 nm. It was worth noting that the λ max shifted in the longer wavelength. This might be due to solvent polarity change, compared with dissolution in ethanol (with a different polarity).

In the spectrum of GO in cyclohexane solution, the *λ* max value was 217 nm, which can be related to the linear diallyl group in GO. However, there was no peak in the spectrum of GO/*β*-CD solvent phase. These results showed that GO was capable of forming an inclusion complex with *β*-CD.

Fourier Transform-Infrared Spectroscopy (FT-IR)

Since the amount of guest molecules included in the inclusion complex does not exceed 10%, the FT-IR spectrum of the guest molecules is usually obscured by cyclodextrin (Kfoury *et al.*, 2014; Marques, 2010).The FT-IR spectra of GO, *β*-CD, GO/*β*-CD are presented in Figure 2. The FT-IR spectrum of *β*-CD showed prominent absorption bands at 3,391.60 cm^{-1} corresponds to O–H stretching vibrations, 2,926.84 cm^{-1} to C-H stretching vibrations, 1,648.31 cm^{-1} to H–O–H bending of water molecules attached to β-CD), and 1,156.48 cm^{-1} to CO and CC stretching and to the COH bending, 1,028 cm^{-1} to C–O–C stretching vibration, 942.19 cm^{-1} to skeletal vibration involving the *α*1,4 linkage, 854.54 cm^{-1}

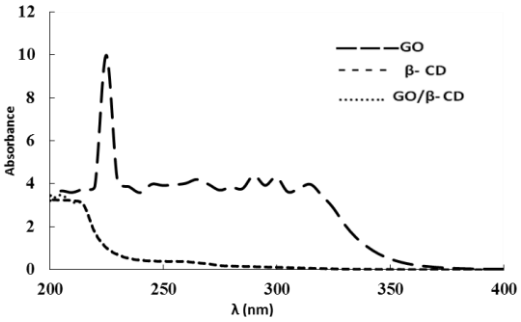

Figure 1. UV-visible spectroscopy of garlic oil (GO) encapsulated by *β* cyclodextrin (β-CD).

to CCH bending and CO and CC stretching, and 580.18 cm^{-1} to the skeletal vibration (Wang *et al.*, 2011; Ding *et al.*, 2013; Chin *et al.*, 2015). In the *β*-CD spectrum, Nikolic *et al.* (2004) perceived (C–O) and (C–O– C) bands at 1,156 and 1,029 cm^{-1}, and Toro-Sa´nchez *et al.* (2010) reported only one band at 2,929 cm^{-1}. Ayala-Zavala *et al.* (2008) also observed the same peaks in the region between 3,400-1,000 cm^{-1} (3,385, 2,925, 1,660, 1,368, 1,158 cm^{-1}). NurAin *et al.* (2011) perceived the 3,400, 2,925, 1,627, 1,343, 1,158, 1,029 cm^{-1}.

The FT-IR spectrum of GO consisted of the prominent absorption bands of asymmetric stretching vibration of $=CH_2$ (3,078.59 cm^{-1}), of C–H stretching (3,008 cm^{-1}), of symmetrical stretching vibration of $=CH_2$ (2,975.74 cm^{-1}), and of $–CH_2–$ stretching (2911.25 cm^{-}). The very intense peak at 1,634.35 cm^{-1} is attributed to C=C stretching vibration of the allyl group. The peak at 1,419.37 cm^{-1} may be referred to the stretching $–CH_2–$ group, while $CH_2=CH–$ stretching is shifted to 1,217.33 cm^{-1}. The other very intense peak at 905.87 cm^{-1} is attributed to C–S–C stretching vibration. Also, the IR spectrum displayed the S–C absorption at 721.49 cm^{-1} and S–S absorption located at 476.52 cm^{-1} (Wang *et al.*, 2011). Ayala-Zavala *et al.* (2008) also observed the same peaks in the region between 3,100- 2,900, and 1,700-1,000 cm^{-1}.

The absorption bands at 3,391.60, 2,926.84, 1,648.31, and 942.19 cm^{-1} of *β*-CD were shifted towards these lower frequencies at 3,370.42, 2,923.46, 1,642.34, and 939.33 in GO/*β*-CD. These might be due to the formation of intra-molecular hydrogen. The bands located at 3,432, 3,078, 2,361, 1,292, and 478 cm^{-1} of GO had totally disappeared. The GO bands were almost

[DOR: 20.1001.1.16807073.2017.19.1.10.5]

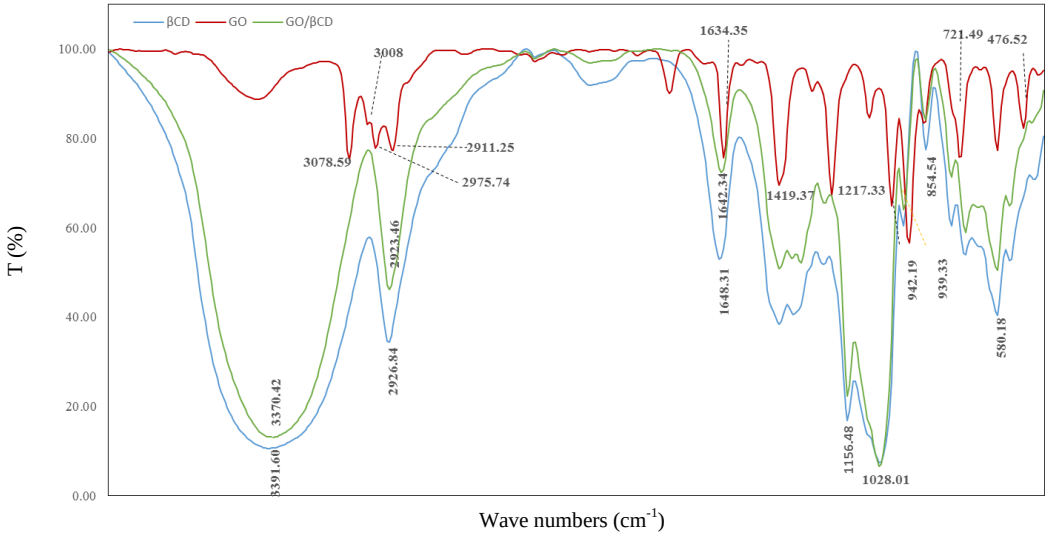

Figure 2. The FT-IR spectrum of *β*-CD (blue spectrum), GO (red spectrum) and GO/*β*-CD complex(green spectrum).

completely obscured by very intense and broad *β*-CD bands (Ayala-Zavala *et al.*, 2008).

Differential Scanning Calorimetry (DSC)

The formation of the GO/*β*-CD inclusion complex was studied by obtaining thermograms concerning GO, *β*-CD, and GO/*β*-CD (Figure 3). DSC can be used to verify inclusion complex formation. When guest molecules were inserted into *β*-CD cavities, their melting, boiling, or sublimation points generally shifted to a different temperature, or disappeared. The thermogram of *β*-CD showed a wide endothermic peak at 90.2°C. The broad endothermic peak was related to desorption of water molecules that were adsorbed to the surface of cyclodextrin

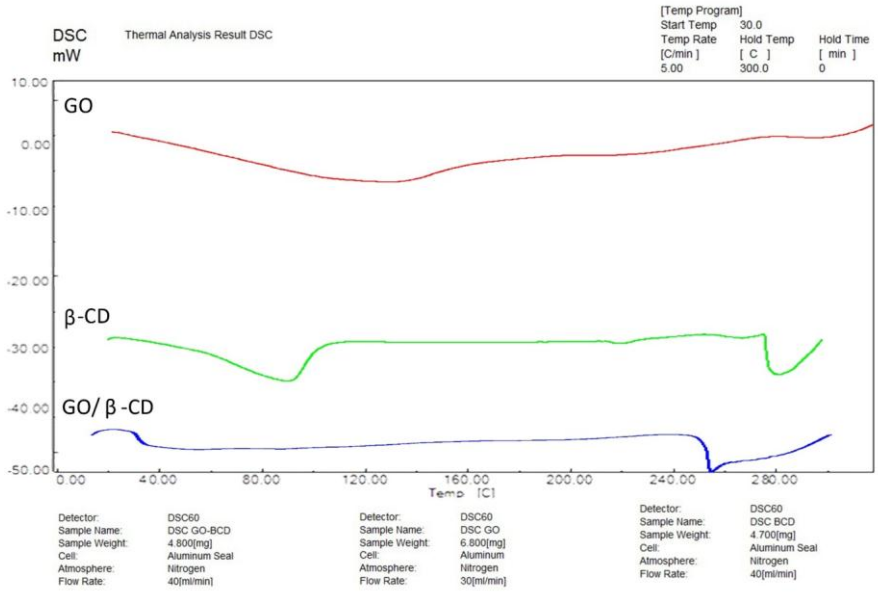

Figure 3. The DSC thermograms of *β*-CD (green), GO (red) and GO/*β*-CD complex (blue).

[DOR: 20.1001.1.16807073.2017.19.1.10.5]

molecules (Marini *et al.*, 1996). There were two endothermic peaks at 222.5 and 280°C. Zhang *et al.* 2015 observed a broad endothermic peak from 72-113°C (with the maximum peak at 83°C) and a small endothermic peak at about 226°C. According to Giordano *et al.* (2001), *β*-CD may exist in different crystal forms and some of them may, more or less readily, transform into each other depending on different ways of preparation methods and the following hydration levels. In the inclusion complex, the shift of *β*-CD peak to low temperature and broadening were the evidence of a reduction in ΔH and a disorder happened in the water molecules inside *β*-CD cavity, which was probably caused by the process of forming inclusion complex (Kfoury *et al.*, 2014). The results suggested that a certain fraction of water molecules binding to *β*-CD were replaced by GO molecules, which meant that GO was successfully included into the *β*-CD cavity.

A different pattern in the thermogram of the GO/*β*-CD complex was observed by Wang *et al.* (2011). The endothermic peak at about 127°C originally in the *β*-CD was slightly shifted to a higher temperature of 131°C for the inclusion complex system due to a major interaction between GO and *β*-CD.

Two exothermic peaks at 128 and 280°C for GO were related to its oxidation, and not present in the DSC scan of the GO/*β*-CD complex indicate protecting GO from oxidation and it indirectly confirms formation of GO's inclusion complex. The endothermic peak at about 280°C originally in the *β*-CD was slightly altered to a lower temperature of 250°C for the inclusion complex system, which could be due to a major interaction between GO and *β*-CD.

X-Ray Diffractometry (XRD)

Beta-CD complexation in powder or microcrystalline states can be detected by XRD. When a true inclusion complex is formed, the diffraction pattern of the complex can be clearly distinct from that of the superimposition of each of the components (Veiga *et al.*, 1996). The diffraction pattern of GO showed non-crystalline nature, without intense and sharp peaks (Figure 4- red spectrum). Some sharp peaks at the diffraction angle of 2θ 8.98, 10.63, 12.43, 19.49 and 24.21° indicated crystalline nature of *β*-CD (Figure 4- blue spectrum), which disappeared in the GO/*β*-CD sample (Fig 4 green spectrum). Only a few new sharp peaks at diffraction angles of 2θ 5.58, 6.86, 11.61, 17.95, and 20.63° were in the X-ray diffractogram of the complex sample, suggesting the formation of the GO/*β*–CD. Disappearance of sharp peaks at a diffraction angle of 2θ between 21 and 34 could implicate elimination of some of *β*–CD in the crystalline state. These implied the presence of new solid crystalline phases in inclusion complex (Figure 4- green spectrum).The data of X-ray diffraction confirmed the results of FT-IR and DSC. Similar results were also found in some other studies (Wang *et al.*, 2011; Zhang *et al.*, 2015).

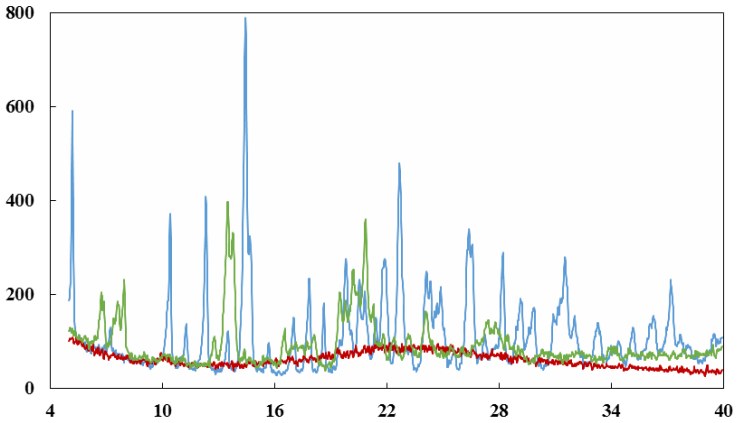

Figure 4. The X-ray diffraction pattern of GO (red spectrum), β-CD (blue spectrum) and GO/β-CD complex (green spectrum).

[DOR: 20.1001.1.16807073.2017.19.1.10.5]

Morphological Analysis

The morphological characteristics of *β*-CD and its inclusion complex with GO are presented in Figure 5. There were drastic changes in particle size and shape among *β*-CD and inclusion complex. The particles of *β*-CD were present in rectangular shape, in agreement with Zhang *et al.* (2015), and probably ascribed to the accumulative crystallization of *β*-CD. Nevertheless, the inclusion complex appeared in very tiny particles with small aggregates. After magnifying to 40,000 times, the inclusion complex showed up as particles of multiangular shape, which was also observed by Zhu *et al.* (2014). The results indicated that the addition of GO would disturb the accumulative crystallization of *β*-CD. In the process of forming inclusion complex, the interference might become deeper. The surface morphology of the samples was clearer when the magnification was increased. The sample of *β*-CD existed in amorphous, irregular crystal which was in accordance with Fauziah *et al.* (2013). The inclusion complex was structurally distinct from *β*-CD. The shapes and sizes of *β*-CD particles were different from those of GO/*β*-CD, which also confirmed the inclusion complex formation of GO and *β*-CD.

Release of GO from the Produced Inclusion Complex

Effect of Medium pH

In pure aqueous solutions, the half-life ($t_{1/2}$) for ring-opening of *β*–CD has been reported to be approximately 15 hours at 70°C and a pH of 1.1, while, *α*-CD is approximately 1.5-times more stable and γ-CD is approximately 1.5-times less

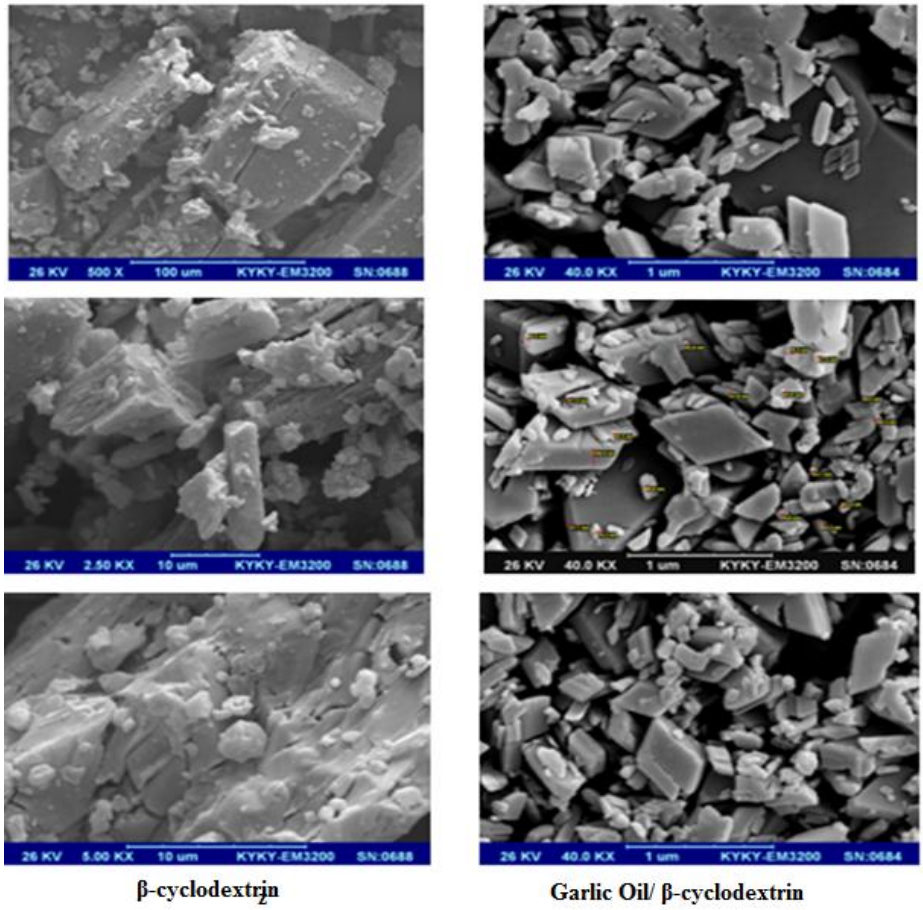

Figure 5. The SEM photographs of *β*-CD and GO/*β*-CD.

[DOR: 20.1001.1.16807073.2017.19.1.10.5]

stable than *β*-CD. However, the formation of inclusion complexes significantly enhances the chemical stability of CDs (Kurkov and Loftsson, 2013). *In vitro* release profile of GO from the GO/*β*-CD complex at different pH (1.5, 4, 5.5, and 6.5) at 37°C is shown in Figure 6. The maximum and minimum release of GO after two days were 36.59% at pH 6.5, and 1.12% at pH 4, respectively. After 6 days, the release of Go at pH 1.5 and 4 were 41 and 2.74%, respectively. Usually, once a microcapsule is submerged in a solution, the two processes of disintegration and dissolution lead to the release of its content. The particles that are released by disintegration are dissolute. These two processes actually occur simultaneously. Dissolution is a slower process than disintegration, depending on the different parameters such as particle size, pH-solubility profile, and surface affinity for the surrounding medium and on the hydrophilic–hydrophobic properties of the encapsulant (Paramera *et al.*, 2011). Wang *et al.* (2011) showed that the release of GO was found to be 19.2, 50.7, and 100% after 2, 4, and 12 hours, respectively, at 37°C and pH 1.5. The results might imply that the steric hindrance of *β*-CD torus protection against evaporation after GO was included in the cavities of *β*-CD, and the release rate of GO depended on the treatment temperature and time considerably. Ayala-Zavala and Gonz´alez-Aguilar (2010) observed that nearly 70% of GO was released from capsules after 5 weeks exposure to 100% Relative Humidity (RH).

Simulated Human Gastrointestinal Tract

The release profile of GO in simulated human gastrointestinal tract (SGF, SIF, mixture of SGF and SIF, and SCF) at 37°C is shown in Figure 7. The maximum and minimum release of GO were in colon (10.29%, after 120 minutes), and stomach (0.60%, after 30 minutes), respectively. After 120 minutes, release of GO in SIF was less than half of the mixture of SGF and SIF. Beta-CD is not absorbed in the upper gastrointestinal tract because of its resistance to salivary and pancreatic amylases and metabolized by the enzymes produced by colon microflora (Zuidam and Nedović, 2010). Conventional dissolution test is less likely to simulate (by USP dissolution apparatus) performance of colon system because of colon's different environment such as scarcity of fluid, reduced motility and presence of microflora. Nieddu *et al.*, (2014) studied thymol release from thymol–*β*-cyclodextrin

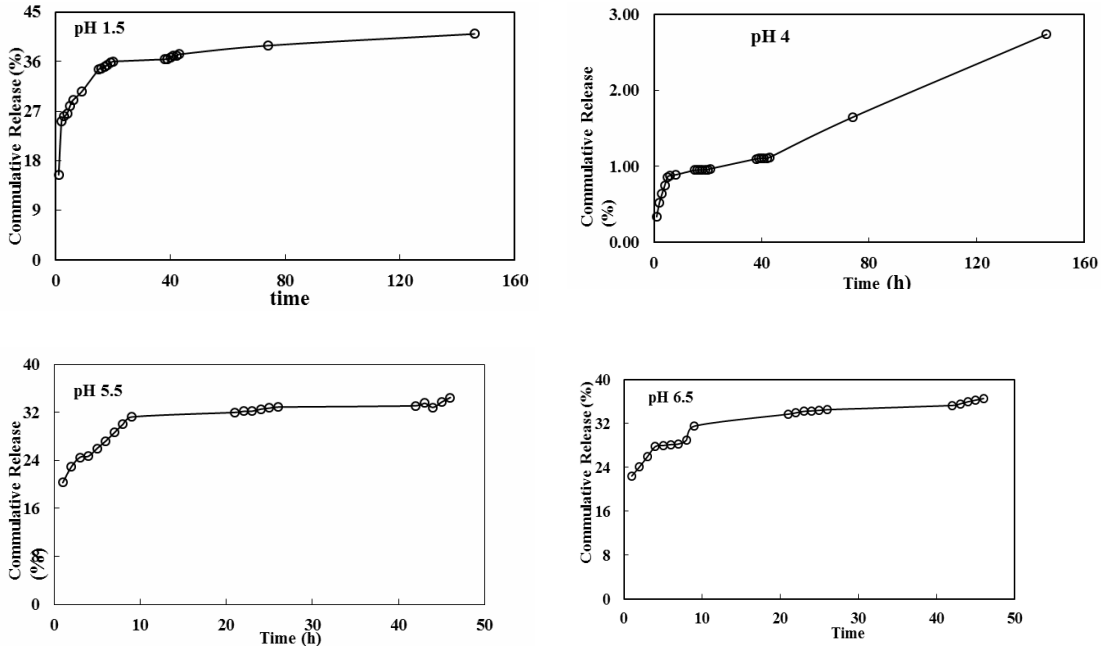

Figure 6. Release profile of GO from the GO/*β*-CD complex at different pH.

[DOR: 20.1001.1.16807073.2017.19.1.10.5]

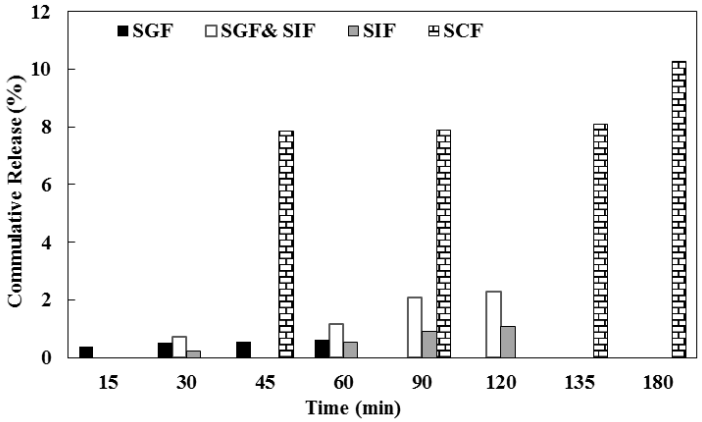

Figure 7. Release profile of GO from the GO/*β*-CD complex in simulated human gastrointestinal tract.

complex in different situations i.e. SGF (containing hydrochloric acid, pH= 1.2) and SIF (adding 0.2M trisodium phosphate dodecahydrate solution to SGF, pH= 6.8). They showed that thymol–*β*-cyclodextrin complex was detained on the surface of the intestinal mucosa, and *β*-cyclodextrin accelerated the in vivo thymol absorption rate compared with the free drug.

CONCLUSIONS

The results of this study showed that GO could form complex with *β*-CD by using the co-precipitation method. Optimum conditions for encapsulation were as follows: temperature: 35°C, core/wall: 8/100, and wall/solvent: 5.5/100. The results of UV–visible spectroscopy, FT-IR, DSC, and XRD implied that GO/*β*-CD complex had different physicochemical characteristics compared to free GO. The *in vitro* release profile of GO from the GO/*β*-CD complex at different pH (1.5, 4, 5.5, and 6.5) at 37°C showed that the maximum and minimum release of GO after two days were 36.59% at pH 6.5, and 1.12% at pH 4, respectively. In simulation of gastrointestinal tract, release of GO in colon was higher than stomach.

ACKNOWLEDGEMENTS

This work was supported by the grant from the research council of Tarbiat Modares University. As Garlic Oil (GO) was kindly supplied by Magnolia Flavor and Fragrance Company, the authors should be grateful for its kindness.

REFERENCES

1. Adams, R. P. 2001. Identification of Essential Oil Components by Gas Chromatography/Mass Spectrometry. Allured Publishing Corporation Carol Stream, IL.
2. Anonymous a 2013. http://www.factfish.com/statistic-country/iran.
3. Anonymous b 2016. http://www.fda.gov/Food/IngredientsPackagingLabeling/GRAS/cm154182.htm.
4. Anonymous c 2016, http://www.garlicworld.co.uk/flavour/Analytical%20Review/page2.html.
5. Anonymous d 2013, http://www.garlicoil.cn/en/display.asp?id=104.
6. Ayala-Zavala, J. F. and Gonz´alez-Aguilar, G. A. 2010. Optimizing the Use of Garlic Oil as Antimicrobial Agent on Fresh-cut Tomato through a Controlled Release System, *J. Food Sci.*, **75**: M398- M405.
7. Ayala-Zavala, J. F., Soto-Valdez H., Gonza´lez-Leo´n, A., Lvarez-Parrilla, E., Martı´n-Belloso, O. and Gonza´lez-Aguilar, G. A. 2008. Microencapsulation of Cinnamon Leaf (*Cinnamomumzeylanicum*) and Garlic (*Allium sativum*) Oils in *β*–Cyclodextrin. *J. Incl. Phenom. Macrocycl. Chem.*, **60**: 359- 368.

[DOR: 20.1001.1.16807073.2017.19.1.10.5]

8. Chin, Y. P., Abdul Raof, S. F., Sinniah, S., Lee, V. S., Mohamad, S. and Abdul Manan N. S. 2015. Inclusion Complex of Alizarin Red S with *β*-Cyclodextrin: Synthesis, Spectral, Electrochemical and Computational Studies. *J. Mol. Struct.*, **1083**: 236- 244.
9. Ding, Z., Wu, M., Guo, Q., Yang, X. and Zhang, B. 2013. Encapsulation of a Flavonoid-rich *Allium cepa* L. var. *agrogatum* Don Extract in *β*-Cyclodextrin for Transdermal Drug Delivery. *J. Agric. Food Chem.,* **61**: 4914- 4920.
10. Douiri, L. F., Boughdad, A., Assobhei, O. and Moumni, M. 2013. Chemical Composition and Biological Activity of *Allium sativum* Essential Oils against *Callosobruchus maculates*. *J. Environ. Sci. Toxicol. Food Technol. (IOSR-JESTFT),* **3**: 30- 36.
11. Fauziah, C. I., Zaibunnisa, A. H., Osman, H. and Wan Aida, W. M. 2013 .Thermal Analysis and Surface Morphology Study of Cholesterol: *β*-Cyclodextrin Inclusion Complex. *Adv. Mat. Res.,* **812**: 221- 225.
12. Giordano, F., Novak, C. and Moyano, J. R. 2001. Thermal Analysis of Cyclodextrins and their Inclusion Compounds. *Thermochim. Acta,* **380**: 123- 151.
13. Haroun, A. A. and El-Halawany, N. R. 2010. Encapsulation of Bovine Serum Albumin within *β*-Cyclodextrin/Gelatin-based Polymeric Hydrogel for Controlled Protein Drug Release. *IRBM,* **31**: 234- 241.
14. Hill, L. E., Gomes, C. and Taylor T. M. 2013. Characterization of Beta-cyclodextrin Inclusion Complexes Containing Essential Oils (Trans-cinnamaldehyde, Eugenol, Cinnamon Bark, and Clove Bud Extracts) for Antimicrobial Delivery Applications. *LWT-Food Sci. Technol.,* **5**: 86- 93.
15. Kfoury, M., Auezova, L., Greige-Gerges, H., Ruellan, S. and Fourmentin, S. 2014. Cyclodextrin, an Efficient Tool for Trans-anethole Encapsulation: Chromatographic, Spectroscopic, Thermal and Structural Studies. *Food Chem.,* **164**: 454- 461.
16. Kurkov, S. V. and Loftsson, T. 2013. *Cyclodextrins: Review*. *Int. J. Pharm.,* **453**: 167- 180.
17. Marini, A., Berbenni, V., Bruni, G., Giordano, F. and Villa, M. 1996. Dehydration of *β*-Cyclodextrin: Facts and Opinions. *Thermochim. Acta,* **279**: 27- 33.
18. Marques, H. M. C. 2010. A Review on Cyclodextrin Encapsulation of Essential Oils and Volatiles. *Flavour Frag. J.,* **25**: 313- 326.
19. McLafferty, F. W. and Stauffer, D. B. 1989. *The Wiley/Nbs Registry of Mass Spectral Data.* Wiley, New York.
20. Nieddu, M., Rassu, G., Boatto, G., Bosi, P., Trevisi, P., Giunchedi, P., Carta, A. and Gavini E. 2014. Improvement of Thymol Properties by Complexation with Cyclodextrins: *In vitro* and *in vivo* studies. *Carbohydr Polym* **102**: 393- 399.
21. Nguyen, T. A., Liu, B., Zhao, J., Thomas, D. S. and Hook, J. M. 2013. An Investigation into the Supramolecular Structure, Solubility, Stability and Antioxidant Activity of Rutin/Cyclodextrin Inclusion Complex. *Food Chem.,* **136**: 186- 192.
22. Nikolic, V., Stankovic, M., Kapor, A., Nikolic, L. J., Cvetkovic, D. and Stamenkovic, J. 2004. Allylthiosulfinate.: *β*-Cyclodextrin Inclusion Complex. Preparation, Characterization and Microbiological Activity. *Pharmazie,* **59**: 845- 848.
23. NurAin, A. H., Farah Diyana, M. H. and Zaibunnisa, A. H. 2011. Encapsulation of Lemongrass (*Cymbopogon citratus*) Oleoresin with *β*-Cyclodextrin: Phase Solubility Study and its Characterization. *2nd International Conference on Biotechnology and Food Science*, IACSIT Press, Singapore, *IPCBEE,* **7:** 44-48.
24. Paramera, E. I., Konteles, S. J. and Karathanos, V. T. 2011. Stability and Release Properties of Curcumin Encapsulated in *Saccharomyces cerevisiae*, *β*-Cyclodextrin and Modified Starch. *Food Chem.,* **125**: 913-922.
25. Peggy, A., Ponce Cevallos, P. A., Buera, M. P. and Elizalde, B. E. 2010. Encapsulation of Cinnamon and Thyme Essential Oils Components (Cinnamaldehyde and Thymol) in *β*-Cyclodextrin: Effect of Interactions with Water on Complex Stability. *J. Food Eng.,* **99**: 70- 75.
26. Petrovska, B. B. and Cekovska, S. 2010. Extracts from the History and Medical Properties of Garlic. *Pharm. Rev.***,** **4**: 106- 110.
27. Pu, H., Chen, L., Li, X., Xie, F., Yu. L. and Li, L. 2011. An Oral Colon-targeting Controlled Release System Based on Resistant Starch Acetate: Synthetization,

[DOR: 20.1001.1.16807073.2017.19.1.10.5]

Characterization, and Preparation of Film-coating Pellets. *J. Agric. Food Chem.,* **59**: 5738- 5745.
28. Rainy, G., Sharma, A., Maina, P. and Shukla, R. N. 2014. Study of Chemical Composition of Garlic Oil and Comparative Analysis of Co-trimoxazole in Response to *In -Vitro* Antibacterial Activity. *Int. Res. J. Pharm.*, **5(2):** 97- 101.
29. Saboktakin, M. R., Tabatabaie, R. M., Maharramov, A. and Ramazanov. M. A. 2011. Synthesis and *In vitro* Evaluation of Carboxymethyl Starch–chitosan Nanoparticles as Drug Delivery System to the Colon. *Int. J. Biol. Macromol.*, **48**: 381-385.
30. Santhosha, S. G., Jamuna, P. and Prabhavathi, S. N. 2013. Bioactive Components of Garlic and their Physiological Role in Health Maintenance: A Review. *Food Biosci.*, **3**: 59-74.
31. Seo, E. J., Min, S. G. and Choi, M. J. 2010. Release Characteristics of Freeze-dried Eugenol Encapsulated with *β*-Cyclodextrin by Molecular Inclusion Method. *J. Microencaps.*, **27**: 496- 505.
32. Siow, L. F. and Ong, C. S. 2013. Effect of pH on Garlic Oil Encapsulation by Complex Coacervation. *J. Food Process. Technol.,* **4**: 199-204.
33. Toro-Sa´nchez, C. L. D., Ayala-Zavala, J. F., Machi, L., Santacruz, H., Villegas-Ochoa, M. A., Alvarez-Parrilla, E. and González-Aguilar, G. A. 2010. Controlled Release of Antifungal Volatiles of Thyme Essential Oil from *β*-Cyclodextrin Capsules. *J. Incl. Phenom. Macrocycl. Chem.,* **67**: 431-441.
34. Veiga, F., Teixeira-Dias, J. J. C., Kedzierewicz, F., Sousa, A. and Maincent, P. 1996.Inclusion Complexation of Tolbutamide with *β*-Cyclodextrin and Hydroxypropyl *β* -Cyclodextrin. *Int. J. Pharm.,* **129**: 63- 71.
35. Wang, J., Cao, Y., Sun, B. and Wang, C. 2011. Physicochemical and Release Characterisation of Garlic Oil-*β*-Cyclodextrin Inclusion Complexes. *Food Chem.,* **127**: 1680-1685.
36. Yang, L. J., Ma, S. X., Zhou, S. Y., Chen, W., Yuan, M. W., Yin, Y. Q. and Yang, X. D. 2013. Preparation and Characterization of Inclusion Complexes of Naringenin with *β*-Cyclodextrin or its Derivative. *Carbohyd. Polym.*, **98**: 861- 869.
37. Zhang, W., Li, X., Yu, T., Yuan, L., Rao, G., Li, D. and Mu, C. 2015. Preparation, Physicochemical Characterization and Release Behavior of the Inclusion Complex of Trans-anethole and *β*-Cyclodextrin. *Food Res. Int.*, **74**: 55- 62.
38. Zhu, G., Xiao Z., Zhou R. and Zhu, R. 2014. Study of Production and Pyrolysis Characteristics of Sweet Orange Flavor-*β*-cyclodextrin Inclusion Complex. *Carbohyd. Polym.*, **105:** 25: 75- 80.
39. Zuidam, N. J. and Nedović, V. A. 2010. Encapsulation Technologies for Active Food Ingredients and Food Processing. Springer, New York, 41 PP.

درون پوشانی روغن سیر در بتاسیکلودکسترین: بهینه سازی و خصوصیات آن

خ. خوش طینت، م. برزگر، م. ع. سحری، و ز. حمیدی

چکیده

هدف این مطالعه بهینه سازی شرایط انکپسوله کردن و تولید کمپلکس دربرگیرنده روغن سیر با بتاسیکلودکسترین به روش هم رسوبی است. روش سطح پاسخ انکپسوله کردن روغن سیر با بتاسیکلودکسترین با سه متغیر و سه سطح انجام و شرایط بهینه به این شرح بود: دمای ۳۵ درجه سلسیوس،

[DOR: 20.1001.1.16807073.2017.19.1.10.5]

نسبت هسته به دیواره ۸ به ۱۰، نسبت دیواره به حلال ۵/۵ به ۱۰۰. تشکیل کمپلکس با روش های گوناگونی شامل ماورای بنفش و مرئی ، طیف نورسنج مادون قرمز، پراکنش پرتو ایکس و کالریمتری روبشی افتراقی بررسی شد. تکنیک های طیف نورسنجی و ساختارشناسی میکروسکوپ الکترونی روبشی تشکیل کمپلکس روغن سیر با بتاسیکلودکسترین را تایید کردند. نمایه رهایش برون تن روغن سیر از کمپلکس دربرگیرنده روغن سیر با بتاسیکلودکسترین در پ هاش های گوناگون (۱/۵، ۴، ۵/۵ و ۶/۵) در دمای ۳۷ درجه سلسیوس نشان دادکه پس از دو روز، بیشترین و کمترین میزان رهایش روغن سیر به ترتیب ٪ ۳۶/۵۹ در پ هاش ۶/۵و ٪۱/۱۲ در پ هاش ۴ می باشد. در شبیه سازی مجرای گوارش بیشترین و کمترین میزان رهایش روغن سیر به ترتیب در روده بزرگ (٪۱۰/۲۹) و معده (٪ ۰/۶۰) بود. بنابراین می توان استفاده ازکمپلکس روغن سیر و بتاسیکلودکسترین را در سامانه های امولسیون غذایی مانند سس سالاد و سوسیس را پیشنهاد کرد.

[DOR: 20.1001.1.16807073.2017.19.1.10.5]